Journal of Environmental Management 414 (2026) 130431

Contents lists available at ScienceDirect

Journal of Environmental Management

journal homepage: www.elsevier.com/locate/jenvman

Research article

Spatiotemporal response of urban bike-sharing ridership to weather, air quality, and future climate change in major U.S. cities

Jangho Lee [a,b,*], Max Berkelhammer [a]

[a] Earth and Environmental Sciences, University of Illinois Chicago, Chicago, IL, 60607, USA
[b] Courant Institute School of Mathematics, Computing, and Data Science, New York University, New York, NY, 10012, USA

ARTICLE INFO

Keywords:
Bike-sharing
Climate change
Urban resilience
Air quality
GIS
Green mobility

ABSTRACT

Bike-sharing systems have become an essential component of sustainable urban transport, yet the resilience of system usage to changing environmental conditions remains insufficiently understood. This study provides a comprehensive spatiotemporal assessment of how weather and air quality influence bike-sharing ridership across five major U.S. cities between 2020 and 2024, and how these dynamics may evolve under future climate scenarios. Using generalized additive models, we reveal that primary weather variables mathematically dominate cycling decisions: ridership peaks around 20–25°C, while precipitation consistently suppresses usage. Conversely, air quality exerts a much weaker, secondary influence characterized by a behavioral dichotomy. Invisible, routine pollutants like ozone act as spurious proxies for pleasant weather, whereas physically perceptible hazards—such as acute wildfire smoke in San Francisco—can trigger sharp declines in usage. Hot spot analyses further show that environmental stress dynamically reconfigures spatial activity, driving a "climatic refuge" effect where cycling shifts toward waterfronts during extreme heat. Projecting these sensitivities forward, we show that future warming will enhance annual cycling suitability, particularly in seasonally cold cities, by reducing prohibitive winter days. Collectively, these results provide an integrated framework for understanding micromobility resilience, highlighting that urban cyclists respond primarily to immediate sensory environments rather than abstract health metrics.

1. Introduction

1.1. Bike sharing as sustainable urban mobility

Urban transportation and mobility systems are currently undergoing a profound, rapid, and necessary transformation. As global populations increasingly concentrate within metropolitan regions, cities are forced to confront the compounding crises of escalating greenhouse gas emissions, deteriorating localized air quality, and chronic, economically debilitating traffic congestion (Ding et al., 2025; Gifford and Steg, 2005; Mo et al., 2018; Wang and Zhou, 2017). In response to these multifaceted urban challenges, urban planners and policymakers have prioritized the transition toward low-carbon, active, and shared transportation modalities (Winkler et al., 2023). Within this shifting paradigm, shared micromobility, most notably docked and dockless bike-sharing systems, has emerged as a foundational component of the modern sustainable urban transport network.

Bike-sharing systems have evolved into critical civic infrastructure that provides flexible and affordable mobility options to millions of urban residents (Fishman, 2016; Shaheen et al., 2010). The rapid expansion and adoption of these systems contributes directly to broad climate change mitigation efforts by decarbonizing passenger kilometers traveled (Chapman, 2007; Creutzig and He, 2009). Beyond global climate targets, the localized integration of high-density bike-sharing networks can be linked to the reduction of surface urban heat island intensities through the displacement of combustion engine-generated anthropogenic heat (Lee and Berkelhammer, 2025). Furthermore, the reduction in vehicular exhaust inherently improves localized air quality, while the promotion of active travel yields cascading public health benefits, including enhanced cardiovascular health, lowered blood pressure among habitual users, and fundamentally improved urban livability (Agarwal et al., 2024; Guo et al., 2022).

However, despite these overwhelming socio-environmental benefits, the resilience of bike-sharing systems remains a subject of intense operational scrutiny. Unlike enclosed forms of mass transit or private automobiles, cycling requires direct, unmitigated physical exposure to the ambient atmospheric environment. Consequently, ridership demand

* Corresponding author. Earth and Environmental Sciences, University of Illinois Chicago, Chicago, IL, 60607, USA.
E-mail address: jangho.lee@nyu.edu (J. Lee).

https://doi.org/10.1016/j.jenvman.2026.130431
Received 8 December 2025; Received in revised form 14 June 2026; Accepted 3 July 2026

is highly elastic and sensitive to external meteorological and environmental disruptions (Cortez-Ordonez et al., 2024; Eren and Uz, 2020). Evaluating the long-term viability and spatial resilience of this crucial sustainable transportation mode under the pressures of a changing climate requires a rigorous, multidimensional approach that transcends isolated case studies.

1.2. Literature review

As a fully exposed mode of active transportation, the efficacy of a bike-sharing system in sustaining modal shifts is highly contingent upon the ambient environmental conditions. The decision to cycle is evaluated daily (and often hourly) by the user, requiring a continuous interaction with the physical environment. To synthesize what is presently known and to conclusively justify the research gaps addressed in this manuscript, here we review the triad of environmental determinants governing cycling behavior: meteorological weather, localized air quality, and the macro-level projections of future climate change.

1.2.1. Meteorological stressors: The non-linear dynamics of temperature and precipitation

Weather variables, particularly ambient temperature and precipitation, are recognized in the literature as the most immediate, potent, and highly localized determinants of daily bike-sharing usage (Corcoran et al., 2014; El-Assi et al., 2017; Gong et al., 2024). The relationship between temperature and cycling can be complex, non-linear, and largely dictated by the physiological limits of human thermal comfort. It is widely theorized to follow an inverted U-shape distribution. Warmer temperatures generally encourage cycling adoption and duration up to a specific optimal threshold point. Beyond this threshold, heat stress, which is characterized by excessive sweating, accelerated fatigue, and the physiological dangers of hyperthermia, becomes an overwhelming psychological and physical deterrent (An et al., 2019; Gebhart and Noland, 2014).

One of the most comprehensive syntheses of weather effects is the comparative analysis by Bean et al. (2021). Analyzing nearly 100 million cycling trips across forty cities spanning five distinct global climate zones, the study established that in the vast majority of urban environments, ridership steadily increases alongside temperature until it peaks at approximately 27°C to 28°C, after which usage begins a sharp decline. Furthermore, their multi-city comparison revealed the critical role of regional acclimatization; populations residing in traditionally colder, boreal, or temperate climates exhibit entirely different thermal optimal zones and heat tolerances compared to populations acclimatized to tropical or subtropical zones.

While temperature dictates the overarching, predictable seasonal curve of bike-sharing activity, precipitation acts as an acute, immediate, and nearly universal barrier (Kharaghani et al., 2023; Kim, 2018). The mechanisms by which rain deters cycling are multifaceted: it introduces severe physical discomfort, dramatically degrades road surface traction, impairs both the cyclist's and motorist's visibility, and drastically elevates the perceived and actual risk of traffic collisions. Empirical studies consistently indicate that even marginal accumulations of rainfall can trigger immediate and substantial reductions in network-wide ridership.

1.2.2. Atmospheric stressors: Routine air pollution versus acute visible hazards

In conjunction with the immediate physical sensations of temperature and precipitation, ambient air quality has emerged as a highly critical, yet behaviorally complex, modifier of active travel. Because cycling elevates cardiovascular activity and respiratory rates, cyclists inhale significantly higher volumes of air per minute than sedentary pedestrians or passengers in enclosed, filtered motorized vehicles. This physiological reality forces cyclists to absorb a disproportionately higher burden of ambient urban pollutants (Huang et al., 2024; Raza et al., 2018).

A rapidly expanding body of literature confirms that elevated concentrations of fine particulate matter (PM2.5), ground-level ozone (O3), and carbon monoxide (CO) can act as statistical deterrents to bike-sharing usage (Hong et al., 2022; Liang et al., 2023; Park et al., 2022). However, a critical distinction must be drawn in the literature between measured pollution and perceived pollution. Unlike temperature extremes or heavy rainfall, which are instantly perceptible and demand an instantaneous behavioral response, the insidious health risks associated with routine, baseline urban air pollution (such as standard traffic exhaust) is often invisible and scentless. Consequently, behavioral responses to routine air pollution are heavily mediated by public perception, individual environmental awareness, and the efficacy of public health communication (Kelly et al., 2012; Pascal et al., 2021).

When air pollution crosses the threshold from an invisible metric to an acute, highly visible environmental hazard, the behavioral paradigm shifts drastically. The literature notes that extreme pollution events, most notably the incursion of dense wildfire smoke into urban environments, can degrade visual acuity, induce immediate olfactory discomfort, and create a tangible sensory deterrent. Under these conditions of visible hazard, studies document acute and immediate contractions in active transportation volumes, as the abstract health risk becomes undeniably concrete, prompting users to abandon cycling entirely or seek refuge in enclosed transit modes (Doubleday et al., 2021; Hesseln et al., 2003). Understanding this dichotomy between invisible routine pollution and visible acute hazards is essential for accurately modeling micromobility resilience.

1.2.3. Climate change: Shifting baselines and long-term micromobility resilience

Anthropogenic climate change is fundamentally and irrevocably altering the temporal distribution and intensity of weather patterns globally. Cities are bracing for the intensification and increased frequency of extreme summer heat waves, while simultaneously projecting a systemic contraction in the duration and severity of cold winter seasons. The implications of this shifting climatological baseline for the long-term viability of outdoor, active urban mobility are profound, complex, and highly geographically divergent.

Studies have begun to address this intersection. For instance, the work by Heaney et al. (2019) utilized downscaled climate models specifically for New York City to demonstrate a projection: a warming climate could increase the overall annual volume of bikeshare ridership over the 21st century. This net-positive effect is hypothesized to occur because the anticipated reduction in highly prohibitive, sub-freezing winter days, combined with the temporal expansion of mild “shoulder seasons” (spring and autumn), generates a surplus of cyclable days that mathematically outweighs the ridership losses incurred during the increasingly severe, but temporally concentrated, extreme summer heatwaves.

However, a major limitation of the current literature is the geographic restriction of these projections. It remains insufficiently explored how the climate-driven projections formulated for a specific temperate zone like New York City generalize across a broader spectrum of cities with different baseline climates. Integrating these divergent climate trajectories into a unified analysis is a critical missing link in the macro-level planning of sustainable, climate-resilient mobility infrastructure.

1.3. Research gaps and contributions

Through the synthesis of the aforementioned literature, several pressing research gaps emerge which this study seeks to address.

First, while some studies rely on isolated, single-city case studies (An et al., 2019; Gong et al., 2024; Heaney et al., 2019; Hong et al., 2022; Zheng et al., 2025), the field has also advanced toward multi-city comparative frameworks (Kou and Cai, 2019; Mahajan & Argota Sánchez-Vaquerizo, 2024; Villarrasa-Sapina et al., 2024). However,

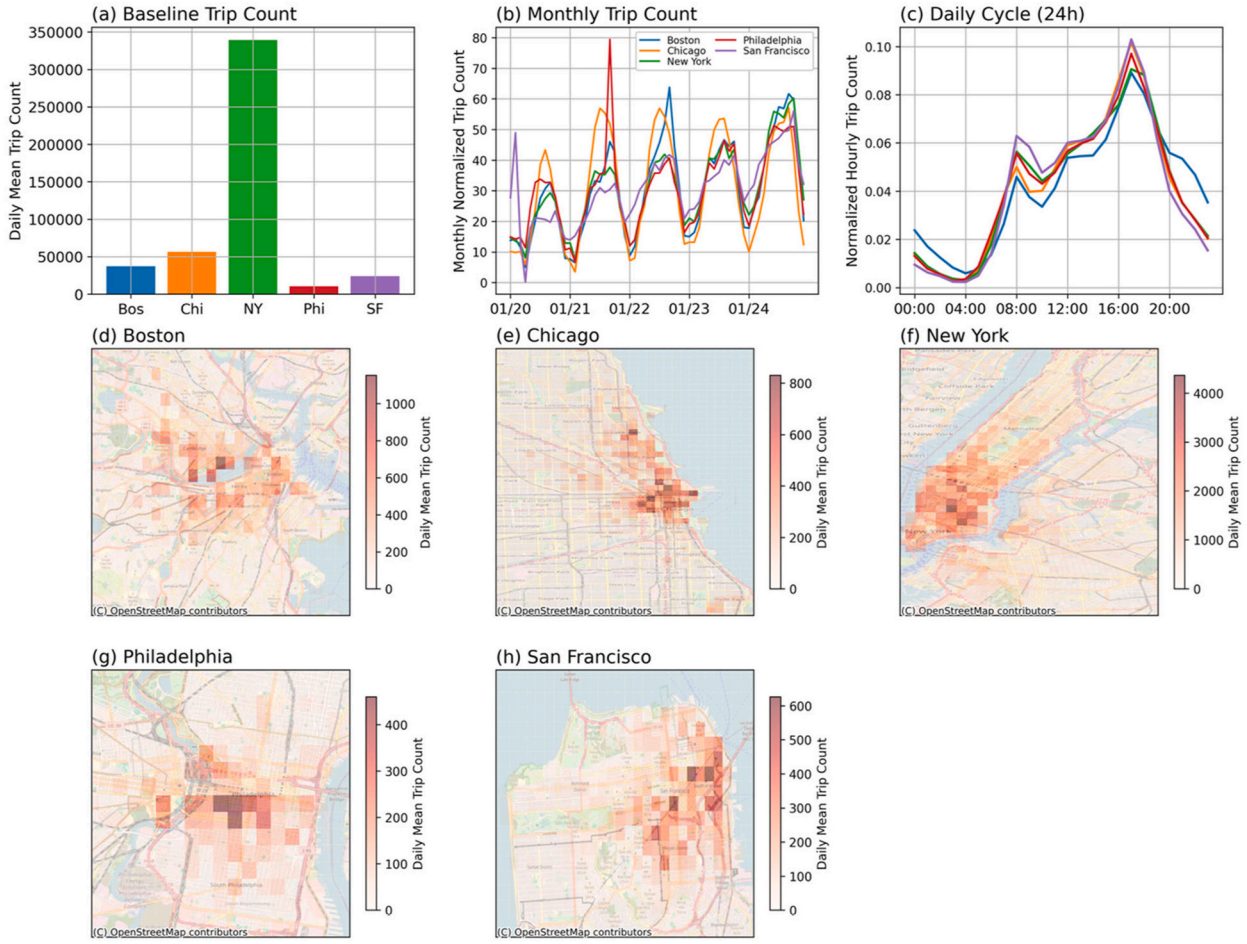

Fig. 1. Spatiotemporal characteristics of bike-sharing usage across five U.S. cities (2020–2024). (a) Daily average trip counts. (b) Normalized monthly ridership. (c) Normalized average 24-h (diurnal) cycle. (d–h) Spatial distribution of mean daily trip counts for Boston, Chicago, New York, Philadelphia, and San Francisco, respectively.

despite this vital progress, a more holistic framework that integrates comprehensive air quality stressors alongside weather and extends these historical sensitivities to project future system resilience under standardized climate change scenarios across contrasting climate zones, is needed.

Second, and perhaps most critically, the spatial dimension of environmental stress on bike-sharing networks must be reconsidered. Static spatial heterogeneity has already been documented in previous studies (Corcoran et al., 2014; Li et al., 2019). Therefore, simply proving that spatial heterogeneity exists is no longer novelty. The underexplored issue is how the spatial concentration of bike-sharing activity is reconfigured under transient environmental stress. When extreme events occur, total ridership may not decline uniformly across the city; instead, statistically significant activity hot spots may persist, disappear, or newly emerge in specific areas. Dense, heat-trapping downtown cores may experience localized network failure, while compensatory cycling activity surges in specific "climatic refuges," such as coastal waterfronts or dense urban park corridors with shade (Cao et al., 2024). Understanding this spatiotemporal reconfiguration is crucial for a complete operational understanding of a network's resilience.

To systematically address these theoretical and methodological gaps, this study provides a comprehensive spatiotemporal assessment of how weather and air quality influence bike-sharing ridership, and how these intricate dynamics will evolve under future climate change scenarios. Deploying an integrated computational framework across five major U. S. cities, this research is driven by three core objectives.

- Temporal Non-linear Analysis across Diverse Climates: Utilizing a flexible statistical model to capture the complex, non-linear responses of ridership to both primary weather variables and diverse air quality metrics.
- Tracking Dynamic Spatial Reconfiguration of Activity Concentration: Moving beyond static spatial heterogeneity by using spatial hot spot analysis to identify where bike-sharing activity hot spots are maintained, lost, or newly formed under environmental stress.
- Future Climate Projections and System Resilience: Projecting these empirically derived historical relationships up to the year 2100 by utilizing high-resolution, bias-corrected climate model projections, providing vital trajectories for urban micromobility resilience in a warming world.

2. Data and method of analysis

2.1. Bike sharing data

This study analyzes publicly available data from bike-sharing systems in five major U.S. cities over a five-year period (January 2020–December 2024). City selection was guided by two main criteria: (1) continuous and reliable operation of the bike-sharing program throughout the study period to ensure temporal completeness, and (2) an average daily ridership exceeding 1000 trips to ensure statistical robustness. The selected cities and their respective systems are Boston (Bluebikes), Chicago (Divvy), New York City (Citi Bike), Philadelphia

(Indego), and San Francisco (Bay Wheels). Cities such as Los Angeles and Washington, D.C. were excluded due to insufficient trip volumes (fewer than 500 trips on most days in Los Angeles) and lack of substantial data coverage (Washington, D.C.).

Each dataset contains detailed trip-level records, including the start and end station coordinates (latitude and longitude) and corresponding timestamps (undocking and docking times). This high-resolution dataset allows for the analysis of spatial usage patterns (by aggregating trip origins and destinations) and their temporal distribution. As illustrated in Fig. 1, the dataset exhibits distinct operational scales and spatio-temporal patterns across the cities. New York City has the highest daily average ridership by a significant margin (approximately 340,000 trips/day), whereas the other four cities have baselines below 100,000 trips/day (Fig. 1a). Looking at the normalized data (divided by daily mean trip count for each city), all systems demonstrate a strong seasonal trend with usage peaking in the summer months (Fig. 1b) and a clear diurnal cycle with bimodal peaks corresponding to morning and evening commuting hours (Fig. 1c). Spatially, bike-sharing activity is heavily concentrated in the dense urban cores of each metropolitan area (Fig. 1d–h).

To preprocess the data, we implemented two filtering steps to remove noise and potential errors. First, spatial outliers were excluded by defining the study area for each city within the 0.5th and 99.5th percentiles of all trip coordinates. This step was implemented to mitigate the influence of GPS positioning errors and extremely long-distance outliers that do not represent typical urban mobility patterns. Second, trips with durations shorter than 60 s were removed, as they are likely to represent false starts or station docking errors. For the main analysis, the filtered trip data were aggregated to a daily temporal resolution and gridded spatially to a resolution of 0.005° in latitude and longitude, corresponding to an approximate grid cell size of 500m × 500m. This spatial resolution was selected to approximate the typical 5-min walking catchment area for bike-sharing stations, balancing the need for fine-grained spatial detail with sufficient data density per cell. To ensure the stability of these results, we conducted comprehensive sensitivity analyses. Testing alternative outlier thresholds (e.g., 1st and 99th percentiles) and alternative spatial grid sizes (e.g., 0.01°) confirmed that the identified spatial hot spot patterns and temporal trends are robust to the choice of preprocessing parameters and spatial units (see Supplementary Section S1 for further details).

2.2. Historical weather and air quality data

Historical daily weather data were sourced from the DayMet V4 dataset (Thornton et al., 2022), which provides gridded climate variables at a 1 km spatial resolution across North America. For this study, we extracted daily total precipitation, specific humidity (sph), and minimum (Tmin) and maximum (Tmax) temperatures. To generate a single representative time series for each metropolitan area, the data from all 1 km grid cells within a 25 km radius of the city center were spatially averaged. The daily mean temperature was calculated as the arithmetic mean of Tmin and Tmax (Thornton et al., 2021), and this, along with total daily precipitation and average daily specific humidity, was averaged across this 25 km radius.

Daily air quality data, including concentrations of carbon monoxide (CO), fine particulate matter (PM2.5), and ground-level ozone (O_3), were obtained from the U.S. Environmental Protection Agency (EPA) Air Quality System. For each city, we used the official city-wide daily summary values, which aggregate observations from multiple standardized monitoring stations to provide a consistent and representative measure of pollutant exposure.

Recognizing that most people are not directly aware of specific pollutant concentrations, we also incorporated the daily Air Quality Index (AQI) for each city, as reported by the EPA (Bishoi et al., 2009; Perlmutt & Cromar, 2019). The AQI offers an integrated and publicly interpretable indicator of overall air quality conditions, facilitating comparison across pollutants and cities. AQI values below 50 are classified as Good, indicating satisfactory air quality. Values between 51 and 100 are considered Moderate, while those from 101 to 150 are categorized as Unhealthy for Sensitive Groups. Values between 151 and 200 are classified as Unhealthy, 201 to 300 as Very Unhealthy, and those exceeding 300 are regarded as Hazardous, posing serious health risks to the entire population.

To test whether ozone and AQI associations partly covary with sunlight, we added DayMet V4 daily shortwave radiation (srad, W/m^2) as a supplementary robustness control. This variable was aligned with the daily ridership and pollution panel and was used only in the additional supplementary models. The baseline historical model remains unchanged. Furthermore, to account for acute wildfire-smoke exposure, we also constructed a daily smoke-exposure indicator using NOAA Hazard Mapping System (HMS) smoke polygons. A city-day was coded as smoke-exposed when an HMS smoke plume intersected the corresponding metropolitan study area. Because wildfire smoke is partly upstream of PM2.5 and AQI, this variable is interpreted as an event-day robustness control rather than as a causal decomposition of particulate pollution. The added-control data construction and HMS smoke-exposure analyses are described in Supplementary Section S2.

Table 1
Global Climate Models (GCMs) and Regional Climate Models (RCMs) from NA-CORDEX used in the projection analysis.

GCM	RCM
CanESM2	CanRCM4
	CRCM5-UQAM
GEMatm-Can	CRCM5-UQAM
GEMatm-MPI	CRCM5-UQAM
GFDL-ESM2M	RegCM4
	WRF
HadGEM2-ES	RegCM4
	WRF
MPI-ESM-LR	RegCM4
	WRF
	CRCM5-UQAM
MPI-ESM-MR	CRCM5-UQAM

2.3. Future weather data

Future climate projections employed in this study were obtained from the North American Coordinated Regional Downscaling Experiment (NA-CORDEX). NA-CORDEX provides dynamically downscaled climate projections generated by coupling multiple Global Climate Models (GCMs) with Regional Climate Models (RCMs), covering the North American domain. Specifically, we utilize projections from 12 distinct GCM-RCM model pairs, as detailed in Table 1, ensuring robust representation of model uncertainty and unforced variability of the climate. GCMs used in this study include CanESM2 (Swart et al., 2019), GEMatm (Šeparović et al., 2013), GFDL-ESM (Dunne et al., 2020), HadGEM2 (Collins et al., 2011), and MPI-ESM (Giorgetta et al., 2013). RCMs used in this study include CanRCM4 (Scinocca et al., 2016), CRCM5-UQAM (Šeparović et al., 2013), RegCM4 (Giorgi et al., 2012), and WRF (Skamarock et al., 2019).

The data utilized in this analysis are available at a daily temporal resolution on the standard NAM-22i grid (approximately 25 km horizontal resolution). To ensure methodological consistency and spatial comparability with our historical observations, the NA-CORDEX projections are bias-corrected and downscaled using the DayMet dataset as the historical baseline period. This downscaling approach aligns the future weather data closely with observed historical climate characteristics. Due to limitations in available datasets, future projections for air quality variables (CO, PM2.5, and ozone) are not included in this analysis.

2.4. Generalized additive models (GAM)

To examine the relationships between shared-bike usage and various environmental factors, we use generalized additive models (GAMs) (Hastie, 2017). GAMs provide a flexible regression framework that allows non-linear responses of the dependent variable to multiple predictors through the use of smooth spline functions. This enables the capture of complex, city-specific behavioral patterns without assuming predefined functional forms.

The baseline model is formulated as:

$$\begin{aligned}\mathrm{Bike}_c = \beta_c + s(\mathrm{temperature}_c) + s(\mathrm{precipitation}_c) + s(\mathrm{CO}_c) + s(\mathrm{PM2.5}_c) \\ + s(\mathrm{Ozone}_c) + s(\mathrm{time}_c) + \mathrm{is\_weekend\_holiday}_c + \varepsilon_c\end{aligned}$$

Here, $\mathrm{Bike}_{c,t}$ represents the normalized daily bike usage (divided by the average daily bike usage) time series for city c. β_c is the intercept, and $s(\cdot)$ term represent the smooth spline functions that describe non-linear effects of environmental variables. The binary variable is_weekend_holiday|| is included as a linear term to account for typical day-of-week differences and holidays. The long-term smooth spline function of $s(\mathrm{time}_c)$ is included to control for the seasonal cycle and long-term changes (4 knots per year). In the GAM framework, a knot defines a point along the time variable where separate spline segments join smoothly, thereby determining the flexibility of the fitted curve. This setting allows the spline to capture broad seasonal and long-term trends—such as linear increases in ridership or shifts during the COVID-19 lockdown—while avoiding overfitting short-term fluctuations. ε represents the residual term.

The GAM is fitted separately for each city using restricted maximum likelihood (REML) to optimize the trade-off between model complexity, predictive accuracy, and generalizability. From these fitted models, partial dependence curves are derived to quantify and visualize the independent contribution of each environmental predictor to daily shared-bike usage. Sensitivity tests were conducted on model parameters, including the number of knots per year, and the results remained consistent across configurations (see Supplementary Material Section S3). This stability reflects the inherent smoothing property of the REML-based estimation, which automatically penalizes overfitting and ensures comparable functional forms across cities.

In addition to the pollutant-specific model above, we constructed an alternative GAM using the Air Quality Index (AQI) as a composite indicator. The AQI model replaces individual pollutant terms ($s(\mathrm{CO}_c)$; $s(\mathrm{PM2.5}_c)$; $s(\mathrm{Ozone}_c)$) with a single smooth function $s(\mathrm{AQI}_c)$, while retaining the same terms for temperature, precipitation, time, and weekend/holiday effects:

$$\begin{aligned}\mathrm{Bike}_c^{\mathrm{AQI}} = \beta_c + s(\mathrm{temperature}_c) + s(\mathrm{precipitation}_c) + s(\mathrm{AQI}_c) \\ + s(\mathrm{time}_c) + \mathrm{is\_weekend\_holiday}_c + \varepsilon_c\end{aligned}$$

Because AQI is derived from CO, PM2.5, and ozone concentrations, this formulation captures their joint influence through a unified metric rather than as separate predictors. To ensure consistency, the smooth terms for temperature, precipitation, and time in the AQI model were fixed to those estimated in the baseline model, so that the AQI term represents the residual contribution of aggregated air quality to cycling behavior. This two-model structure allows direct comparison between the effects of individual pollutants and their combined perceptual or communicative signal as reflected by AQI.

To identify the most relevant thermal comfort metric for cycling, we tested four different temperature-related variables: standard dry-bulb temperature (DBT), wet-bulb temperature (WBT), Heat Index (HI), and a simplified wet-bulb globe temperature (sWBGT). A comparison of GAM model performance using the R-squared (R^2), Akaike Information Criterion (AIC), and root mean squared error (RMSE) indicated that DBT provided the most explanatory power (see Supplementary Section S4). Consequently, DBT was used for all analyses hereafter.

As a robustness check, we also estimated added-control GAM specifications for both the pollutant-specific and AQI model families by including solar radiation and HMS smoke exposure. These models are reported in Supplementary Section S2 for comparison and are not intended to replace the baseline specification.

2.5. Hot spot analysis

To examine how the spatial concentration of bike-sharing activity responds to extreme environmental conditions, we conducted a hot spot analysis based on the Getis–Ord Gi* statistic. This method evaluates the spatial association among neighboring areas to determine whether high or low usage values are clustered in space beyond what would be expected by random chance. In this framework, a hot spot refers to a location where bike usage is significantly higher than that of its surrounding areas, whereas a cold spot represents a cluster of unusually low activity.

We first constructed two composite (average) maps of daily bike usage for each environmental variable. In this context, the daily bike usage for a specific grid cell is explicitly defined as the total aggregate sum of all trip origins (unlocking events) and trip destinations (locking events) that occurred within the boundaries of that cell on a given day. The Normal Days map was then created by averaging this daily usage data from days when the mean temperature fell between the 25th and 75th percentiles of its distribution. The Extreme Condition Days map was created by averaging days when the environmental variable exceeded its 95th percentile (for high extremes such as heat, rainfall, or air pollution) or dropped below its 5th percentile (for cold extremes). These composite maps allow us to capture stable spatial patterns representative of typical versus extreme conditions.

We defined the reference baseline as all non-event days across the entire study period, rather than using seasonally stratified subsets. This methodological choice was made to capture the absolute deviation of ridership patterns from the system's standard operating state. By comparing extreme events against the annual norm, the analysis reflects the total environmental load—the combined influence of seasonality and the specific stressor—providing a more practical assessment of system resilience and infrastructural stress than a seasonally adjusted metric would offer.

The Getis-Ord Gi* statistic was then calculated for each grid cell i on both maps independently. The statistic for a cell i is given as a Z-score:

$$G_i^* = \frac{\sum_{j=1}^{n} w_{ij}x_j - \bar{X}\sum_{j=1}^{n} w_{ij}}{S\sqrt{\frac{\left[n\sum_{j=1}^{n} w_{ij}^2 - \left(\sum_{j=1}^{n} w_{ij}\right)^2\right]}{n-1}}}$$

Where x_j is the usage value for cell j, w_{ij} is the spatial weight between cell i and j, based on Queen contiguity to include all eight surrounding neighbors. $\bar{X}$ is the mean of all cell values, S is the standard deviation of all cell values, and n is the total number of cells.

Cells with a Z-score greater than 1.645 ($p < 0.1$) were classified as statistically significant hot spots, and cells with negative Z-scores of similar magnitude were classified as cold spots. The analysis was performed separately for the Normal and Extreme composite maps. Comparing these two sets of results allowed us to observe how the "hot spots" of bike activity shift spatially when cities face environmental stressors. Importantly, this method focuses not on day-to-day fluctuations in total trip counts but on the relative reconfiguration of activity within each city. In other words, it helps reveal where people ride more or less under weather stress, not simply how many people ride. Conceptually, this analysis captures whether the spatial "centers of activity" remain stable or migrate when environmental conditions become extreme. Rather than simply showing how total ridership changes, the method reveals whether the concentration of use becomes more dispersed, shifts toward specific neighborhoods, or contracts to

particular corridors under stress. In this way, the hot spot analysis provides an interpretable spatial signature of how urban mobility patterns adapt to adverse environmental conditions.

Unlike the GAM framework where all environmental and non-environmental confounders are mathematically controlled as covariates, the spatial hot spot analysis relies on generating composite average maps. Therefore, to rigorously isolate the spatial signature of each environmental stressor in these maps, we applied strict conditional data filtering. When analyzing the spatial impact of extreme heat, days where precipitation occurred were excluded from the map generation process. This mapping-specific filtering helps ensure that the observed spatial reconfiguration patterns are associated with the target stressor under investigation, while avoiding the dominant confounding suppression of rainfall on spatial activity.

Data from the entire study period were aggregated for the spatial analysis. This approach was chosen to maximize statistical robustness and to identify structurally persistent hot spots that exhibit consistent sensitivity to climate stress over the long term, filtering out transient spatial shifts associated with specific short-term periods.

It is also worth noting that while alternative approaches such as Origin-Destination (OD) flow models or Latent Class Models (LCM) could offer valuable insights into network connectivity and static station typologies, they were not employed in this study. Our primary objective was to pinpoint the dynamic spatial shifts of ridership in response to transient environmental forcing (e.g., heatwaves). For this specific purpose, the density-based Getis-Ord Gi* statistic provides a direct and interpretable measure of localized activity concentration, capturing changes in the spatial configuration of bike-sharing activity without the complexity of route reconstruction.

3. Results and discussion

3.1. Temporal effect of environmental factors

To investigate the city-wide temporal dynamics of bike-sharing, we first modeled the spatially aggregated normalized daily ridership volume against various environmental factors using the GAM framework. The partial dependence curves and their 95% confidence intervals (CIs) reveal distinct non-linear relationships, city-specific sensitivities, and varying degrees of statistical uncertainty (Fig. 2).

Temperature (DBT) exerts the most dominant influence on ridership, driving dependence fluctuations spanning an absolute range of approximately 0.8 (Fig. 2a). Usage reaches a maximum at specific optimal temperatures before declining. For Boston, New York, and Philadelphia, this optimal threshold is consistent, peaking precisely between 21.3°C and 21.7°C. Chicago exhibits an optimal temperature shifted higher to 26.4°C, whereas San Francisco displays a distinctly lower peak at 19.2°C. The narrow 95% CI bands across the core temperature ranges indicate high model confidence in these regional adaptations.

Precipitation consistently demonstrates a steep, negative impact on bike usage (Fig. 2b). Ridership peaks at 0.0 mm/h (no precipitation). The initial dampening effect is substantial and uniform; a light rainfall of just 5 mm/h corresponds to a sharp decrease in the normalized ridership index by 0.10 to 0.13 across all five cities.

Before examining specific pollutants, it is critical to contextualize their absolute magnitudes and statistical uncertainties. While temperature and precipitation show dependence swings of up to 0.8 and 0.4, respectively, all air-quality metrics (AQI, ozone, PM2.5, and CO) are

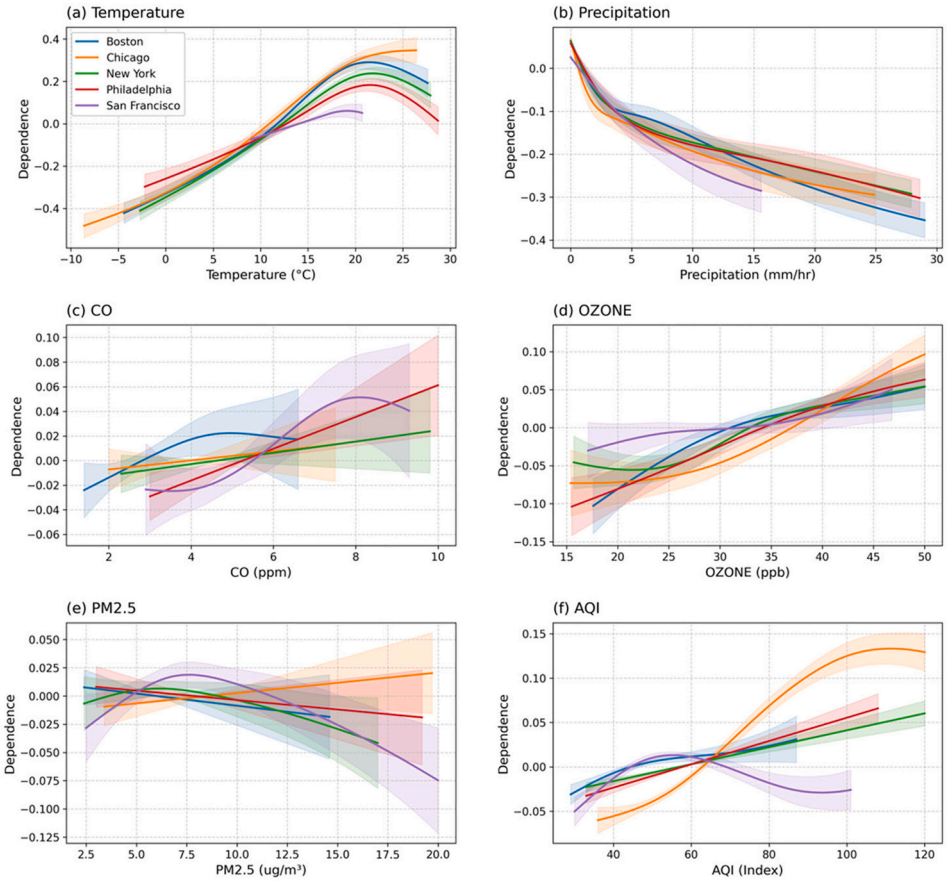

Fig. 2. Partial dependence plots from the city-wide GAMs. The curves illustrate the modeled non-linear relationship between normalized daily ridership and six key environmental variables, holding all other variables constant. The panels show the partial dependence for: (a) Temperature, (b) Precipitation, (c) Carbon Monoxide, (d) Ozone, (e) Fine Particulate Matter (PM2.5), and (f) Air quality index (AQI). 95% confidence intervals (CIs) are shown for all figures as shaded areas.

constrained within a narrower dependence range of approximately −0.10 to +0.13. The 95% CI shaded regions for pollutants also widen at higher concentration tails, reflecting increased uncertainty due to sparse extreme events. This magnitude difference indicates that weather variables show the largest modeled associations with ridership, whereas routine air-pollution associations are comparatively weak and secondary.

Within this narrower scale, ozone concentration shows a positive baseline association with bike ridership in several cities (Fig. 2d). Because ground-level ozone formation is linked to sunlight and stagnant air, this association may partly reflect covariance with favorable outdoor conditions. The supplementary models that add DayMet shortwave radiation show that the 95th percentile level ozone contrast is attenuated in all five cities after the added controls are included (Supplementary Section S2). We therefore interpret the positive ozone association cautiously as photochemical-weather covariance rather than as a direct beneficial effect of pollution.

Similarly, the partial dependence on AQI displays context-dependent baseline associations (Fig. 2f). In several cities, AQI shows a positive baseline association, but the supplementary models indicate that this association is attenuated after adding solar-radiation and smoke controls (Supplementary Section S2). Because AQI can covary with ozone-related photochemical conditions, the positive AQI response should not be interpreted as evidence that poorer air quality directly increases cycling. We therefore interpret the AQI result as a weak and control-sensitive association rather than a direct behavioral response to pollution.

In stark contrast, the response to PM2.5 and AQI in San Francisco highlights the behavioral tipping point where pollution transitions into a physically perceptible hazard. In San Francisco, PM2.5 shows a clearer negative high-tail response, while the AQI response becomes weaker after adding solar-radiation and HMS smoke controls. The diagnostics in Supplementary Section S2 show that high-tail PM2.5 and AQI days frequently overlap with HMS smoke exposure, including 59.21% of top 5% PM2.5 days and 64.47% of top 5% AQI days. Because wildfire smoke, PM2.5, AQI, and weather conditions are closely linked, we interpret this result as event-day robustness evidence rather than a causal decomposition. The interpretation is therefore that acute high-pollution particulate episodes in San Francisco are associated with ridership reductions, while routine pollution effects remain weaker and city-specific.

To empirically evaluate the counterintuitive air-quality signs, we added threshold-specific robustness tests for AQI, PM2.5, and CO in the Supplementary Material. Across 15 city-pollutant combinations (5 cities × 3 air-quality variables), 8 showed no clear adverse or turning threshold and 5 showed statistically non-significant effects below the identified threshold. Two city-specific PM2.5 cases retained negative below-threshold associations, so we avoid interpreting the threshold pattern as a universal behavioral rule (see Supplementary Section S5). Full added-control model comparisons, solar-radiation attenuation results, HMS smoke diagnostics, and threshold tests are reported in Supplementary Sections S2 and S5.

3.2. Spatial effects of environmental factors

While the city-aggregated GAMs reveal the overall temporal response to environmental factors, the hot spot change analysis (Fig. 3) uncovers the spatial dynamics by showing where these changes in bike-sharing hot spots occur. A prominent pattern observed in Boston, Chicago, and New York is the emergence of a "climatic refuge" effect during periods of heat-related stress. In Boston, under extreme heat and high ozone conditions (Fig. 3, a2, a6), new hot spots (red) emerge along the cooler harbor front. Similarly, Chicago sees the formation of new hot spots along its northern lakefront (Fig. 3, b2), and New York exhibits a subtle but similar shift, with new hot spots appearing on the Hudson River waterfront (Fig. 3, c2, c6). The maps provide strong visual evidence that this is not simply new activity, but a spatial reconfiguration of activity concentration. Critically, as these new waterfront hot spots are activated, existing hot spots within the denser, heat-vulnerable urban cores are simultaneously lost (blue). This pattern supports the suggested trade-off: it indicates that essential, utilitarian cycling in established

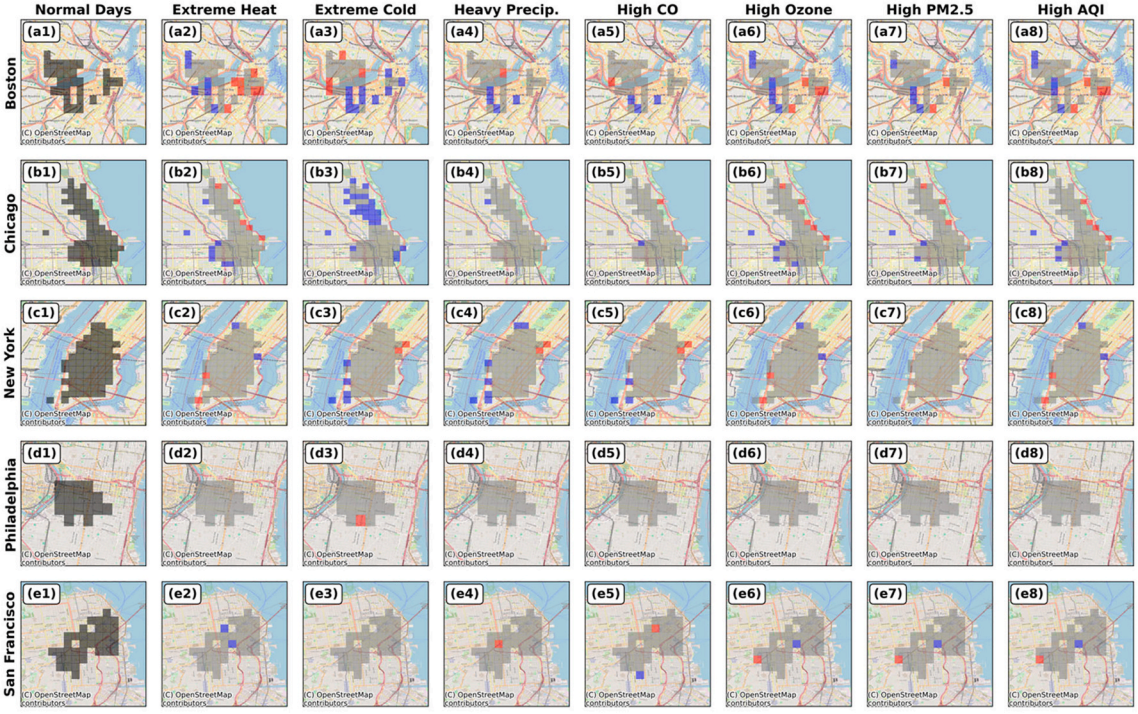

Fig. 3. Hot spot analysis of bike-sharing usage under extreme environmental conditions. Each row corresponds to a city, focusing on areas of concentrated activity. The first column (a1–e1) presents baseline hot spots during Normal Days (dark gray). Subsequent columns (a2–e7) illustrate the spatial patterns observed under each extreme condition, with grid cells classified as Maintained (gray), New (red), or Dispersed (blue) relative to the normal-day baseline.

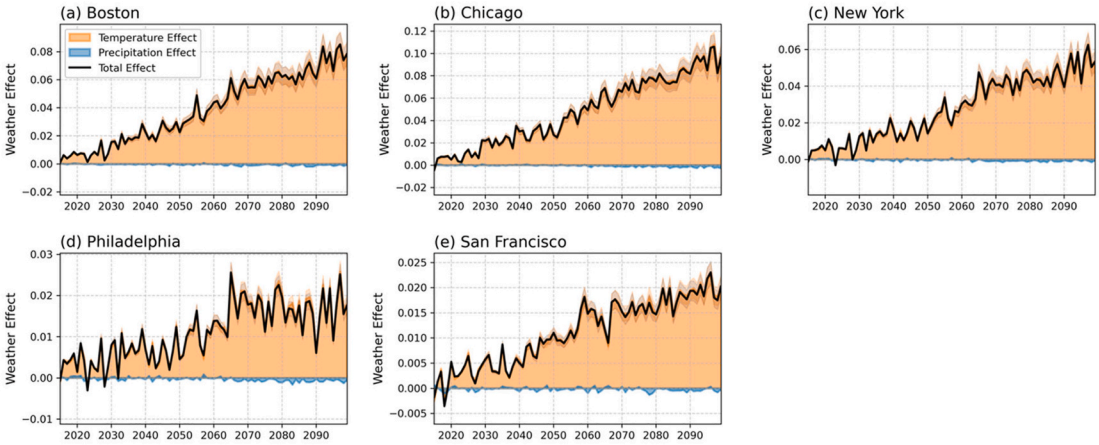

Fig. 4. Projected future temporal trends of the weather-related effect on bike-sharing ridership under the RCP8.5 scenario. Panels show the projected partial effects for (a) Boston, (b) Chicago, (c) New York, (d) Philadelphia, and (e) San Francisco. In each panel, the contributions from projected changes in temperature (orange area) and precipitation (blue area) are shown, along with their total combined effect (black line). The 95% confidence interval is plotted as a shaded band, based on the spread between different NA-CORDEX simulations.

downtown corridors may decline or be disrupted, while recreational or comfort-seeking cycling simultaneously increases or shifts towards areas with more tolerable microclimates, such as those near water bodies.

In contrast, extreme cold triggers a significant hot spot decrease in Chicago (Fig. 3, b3), and the spatial pattern is qualitatively different from the heat-related substitutions. The large, dense usage area in the downtown area visually different. What makes this severe contraction distinct is the lack of compensatory activity; the map is overwhelmingly dominated by lost hot spots, with a near-total absence of new hot spots emerging elsewhere. This suggests that rather than the network adapting or changing, its central hub experiences a net failure under these conditions. The numerous grid cells becoming inactive (dispersed) are not replaced, indicating the downtown core's function as a biking hub is highly vulnerable to winter conditions, possibly as commuters (who might otherwise cycle) switch to enclosed or underground transit options.

The remaining cities, Philadelphia and San Francisco, demonstrate spatial resilience to most environmental stressors, though they achieve this stability through visibly different mechanisms. Philadelphia's compact hot spot cluster is exceptionally stable, showing almost no significant change—minimal red or blue cells—across all extreme conditions (Fig. 3, d1-d7). This lack of dynamics suggests the spatial structure of the core biking activity within this cluster is highly inelastic to environmental factors, continuing largely uninterrupted. San Francisco's hot spot network also maintains its overall structure but shows slightly more dynamic reconfigurations. Rather than being static, its map shows a consistent churn of hotspots (Fig. 3, e1-e7). This pattern is revealed to be a process of local displacement: some cells disperse while new ones emerge nearby. This mechanism allows the network to continuously adapt and re-adjust at a micro-scale in response to various stressors, maintaining its overall integrity without shifting wholesale or failing.

Finally, the High AQI scenario (Fig. 3, a8–e8) reveals spatial patterns that resemble those observed under high ozone conditions. However, the supplementary robustness models show that positive AQI and ozone associations are attenuated after controlling for solar radiation and smoke exposure (Supplementary Section S2). Thus, the spatial similarity is interpreted cautiously as reflecting overlap with warm, sunny, ozone-forming conditions rather than a direct preference for poorer air quality. A sensitivity test regarding the grid size dependency of the hot spot analysis is provided in Supplementary Material Section S1.

3.3. Future projections of weather effects on bike-sharing

To understand the long-term implications of climate change on urban cycling, the fitted GAMs were coupled with future climate projections from the NA-CORDEX ensemble under the RCP8.5 high-emissions scenario. This final stage of the analysis projects how the weather's influence on the suitability of urban cycling is likely to evolve over the 21st century. The results, illustrated in Fig. 4, reveal the potential for a significant and systematic shift in the usage of bike-sharing across all five cities. The most prominent finding is a robust positive trend in the total weather effect (black line) for all metropolitan areas. This suggests that as the century progresses, the net influence of weather will become a significant positive contributor to bike-sharing ridership. This upward trend is overwhelmingly driven by the projected changes in temperature (orange area). The non-linear relationship established in our GAMs (Fig. 2a) indicates that the primary benefit of a warming climate is not the warming of already-hot summers, but rather the reduction of cold, prohibitive days during the winter and the expansion of pleasantly warm conditions in the spring and fall. This expansion effectively lengthens the viable period for comfortable cycling each year. In contrast, the projected changes in precipitation patterns (blue area) have a negative, but negligible long-term impact.

Furthermore, the magnitude of this positive trend is highly heterogeneous and directly linked to the cities' baseline climates. Seasonally cold cities such as Chicago and Boston are projected to experience the largest percentage gains. By 2100, the weather's partial effect in these cities is projected to increase the ridership index by 8 to 10% (which corresponds to +3000 and 5000 daily rides). This amplified effect occurs because these cities are currently the most constrained by cold weather; therefore, they have the most to gain from the reduction of cold days. Conversely, the positive impact is less pronounced in temperate cities like San Francisco (2%, +500 daily rides). Nevertheless, since New York has the highest baseline bike counts (Fig. 1a), it has the largest absolute increase in daily bike counts (+20,000 by year 2100) despite its moderate increase in normalized values (5%).

It is important to emphasize that these projections are based solely on future weather variables (temperature and precipitation), as reliable, downscaled future projections for air quality were not available for this analysis. The projected positive trend in ridership suitability is not a consequence of hotter summers; our GAMs show that extreme heat can be a deterrent. Instead, the primary driver is the significant reduction in

the number of cold, prohibitive days during the winter and the expansion of optimal riding temperature conditions in the spring and fall.

4. Summary and conclusions

4.1. Summary of the work

This study provides a comprehensive analysis of the spatiotemporal response of bike-sharing systems in five major U.S. cities to multiple environmental stressors, including both weather and air quality. By integrating city-wide temporal non-linear regression (GAM), detailed spatial hot spot analysis (Getis-Ord Gi*), and future climate projections, we aimed to understand the complex and heterogeneous ways in which urban bike sharing mobility systems function under environmental pressure.

Our findings reveal several key insights. First, our temporal analysis confirmed that primary weather variables are dominant drivers of daily ridership. Temperature exhibits a distinct non-linear effect, with an optimal range for cycling between 20°C and 25°C across most cities (Heaney et al., 2019; Zheng et al., 2025). Precipitation acts as a universal deterrent, with even light rainfall causing a sharp and immediate decline in usage (Kharaghani et al., 2023; Kim, 2018). In contrast, air pollutants exhibit a weaker and more complex influence (Hong et al., 2022; Liang et al., 2023; Park et al., 2022). The heterogeneous responses to PM2.5, for example, show a distinct negative trend in San Francisco that is potentially linked to heightened public awareness during wildfire smoke events. Moreover, AQI, which integrates multiple pollutants into a single public-facing metric, displayed mixed associations across cities, reflecting how perceived rather than measured air quality can influence cycling behavior. These findings highlight that the impact of air quality on cycling usage, unlike direct weather effects, is often mediated by local context and public perception. This distinction is important because cycling under heavy air pollution can pose serious health risks (Huang et al., 2024; Raza et al., 2018; Schepers et al., 2015), yet poor air quality is often not directly perceptible in the way temperature or precipitation is. Therefore, the implementation of more active and timely air quality alert systems could play a crucial role in informing and protecting urban cyclists.

Second, our hot spot analysis uncovered distinct city-specific spatial adaptations. We identified a “climatic refuge” effect, where activity shifts towards water bodies during hot conditions, especially in Boston and Chicago. This pattern was most prominent during extreme heat but was also observed, albeit more weakly, during days with high ozone, reinforcing the likelihood that these effects are entangled with temperature. Philadelphia offers a useful warmer-city contrast, with a nearly flat future weather-effect trajectory and no extensive shoreline refuge, suggesting that already warm inland systems may experience both smaller climate-suitability gains and fewer spatial refuge responses under heat stress. We also highlighted the dramatic decrease of Chicago's core hot-spot network and the notable resilience of the networks in Philadelphia and San Francisco, underscoring that the spatial response to environmental stress is geographically specific (Bean et al., 2021; Sarkar et al., 2015; Villarrasa-Sapina et al., 2024).

Finally, by coupling these observed relationships with climate projections, we find that a warming climate is projected to significantly increase the number of days with weather suitable for cycling. This net positive trend is not driven by hotter summers but by the reduction of cold, prohibitive days, which effectively expands the duration of favorable cycling conditions in the spring and fall. The impact is greatest in seasonally cold cities like Chicago and Boston, suggesting a future convergence in the baseline weather suitability for cycling across different North American climates.

4.2. Contributions and implications

The contributions of this work are twofold. Methodologically, we develop an integrated framework that combines GAM analysis with spatial hot spot analysis to evaluate the spatiotemporal resilience of urban bike-sharing systems under multiple environmental stressors. This approach allows for the characterization of complex, city-specific responses that are often obscured in single-variable (Ahn et al., 2022; Noland, 2021), linear and fixed-parameter regression (Kim, 2018; Wessel, 2020) analyses. By capturing non-linear and spatially heterogeneous relationships between environmental factors and shared bike usage, our framework provides a more nuanced understanding of urban mobility dynamics than conventional linear models.

From a practical standpoint, our findings provide critical insights for urban planners and policymakers. The strong non-linear effect of temperature highlights the importance of designing cycling infrastructure and outreach programs that support thermal comfort, such as shaded routes, seasonal bike lanes, and heat mitigation strategies (Cao et al., 2024; Chen et al., 2020; Mateo-Babiano et al., 2016). The discussion on air quality further suggests that simply providing pollution data may not be sufficient to change mobility behavior. The stronger behavioral response observed in San Francisco, where wildfire smoke makes pollution visibly perceptible, indicates that public health messaging must go beyond data dissemination (Doubleday et al., 2021; Hesseln et al., 2003). Communicating the invisible risks associated with pollutants such as PM2.5 or CO in a more tangible and relatable manner may be essential to influencing travel decisions and protecting public health (Kelly et al., 2012; Pascal et al., 2021).

4.3. Limitations and future work

While this study provides a robust multi-city framework, several limitations highlight critical avenues for future research. First, our statistical models do not explicitly incorporate high-resolution spatial data regarding the built environment, such as the presence of protected bike lanes, urban canopy cover, or station network density. As a result, we cannot account for how physical infrastructure might mediate environmental effects. For example, shaded bike lanes may significantly mitigate heat stress, while physically protected lanes may reduce the perceived danger of riding in light rain. Consequently, our findings represent the average environmental sensitivities across the existing, highly heterogeneous infrastructure of each city. It remains unclear whether the observed spatial shifts are driven purely by environmental preferences or are constrained by the pre-existing network of cycling infrastructure.

Relatedly, our spatial analysis relies exclusively on trip origin and destination data rather than the actual routes taken by cyclists. This simplification assumes that environmental conditions at the trip endpoints are representative of the entire journey, potentially overlooking how route choices through diverse microclimates actively mediate a rider's exposure to environmental stressors. Furthermore, to maintain methodological consistency with the 25 km grid of the NA-CORDEX future climate projections, our historical weather and air quality variables were spatially averaged across each metropolitan area. Consequently, our analysis captures the network response to macro-level environmental forcing (such as regional heatwaves or city-wide smoke plumes) but cannot resolve the influence of highly localized microclimates or street level pollution gradients. Finally, our dataset is restricted to public bike-sharing records and does not reflect the behaviors of private bicycle owners, whose travel patterns and demographic profiles may differ. Future research must integrate granular built environment variables, high resolution urban meteorological networks, and route-level inference models to disentangle how urban infrastructure amplifies or buffers the impacts of climate and weather on active mobility.

Methodologically, as an observational study, our framework is designed to capture complex, non-linear spatiotemporal associations rather than to establish strict causal relationships. Although our models rigorously control for concurrent environmental variables and key temporal factors, unobserved confounding variables—including the detailed socioeconomic characteristics of individual riders—may still

exist. Additionally, the spatial aggregation of data across the entire study period, while effective for identifying structural vulnerabilities, may obscure transient compositional shifts that occurred during the COVID-19 pandemic (e.g., the relocation of activity from commercial hubs to residential areas). Future studies should leverage advanced causal inference designs to definitively isolate the causal effects of environmental and socioeconomic factors on micromobility adoption.

Finally, our long-term climate projections assume that the current sensitivity of ridership to meteorological variables will remain static over time, and they are confined exclusively to primary weather variables due to the current limitations in highly downscaled future atmospheric chemistry models. As such, our projections do not account for future localized changes in air quality. This is a vital limitation because the environmental benefits of a warming climate (e.g., fewer freezing winter days) could be severely counteracted by climate-driven air quality degradation, such as spikes in PM2.5 from increased wildfire frequency. Furthermore, this static approach does not account for potential societal adaptations, such as the widespread adoption of e-bikes, extensive infrastructure expansion, or human behavioral acclimatization to higher temperatures. Therefore, our projections should be interpreted as a baseline assessment of climate-driven thermal pressure on the current system configuration, rather than a precise forecast of future demand. Incorporating these air quality risks and adaptive dynamics, alongside finer-grained socioeconomic indicators, will be essential for developing a comprehensive understanding of urban micromobility resilience in a warming world.

CRediT authorship contribution statement

Jangho Lee: Conceptualization, Data curation, Formal analysis, Investigation, Methodology, Project administration, Resources, Software, Supervision, Validation, Visualization, Writing – original draft, Writing – review & editing. **Max Berkelhammer:** Funding acquisition, Supervision, Writing – review & editing.

Declaration of competing interest

The authors declare that they have no known competing financial interests or personal relationships that could have appeared to influence the work reported in this paper.

Acknowledgements

This material is based upon work supported by the U.S. Department of Energy, Office of Science, Office of Biological and Environmental Research's Urban Integrated Field Laboratories CROCUS project research activity, under Award Number DE-SC0023226.

Appendix A. Supplementary data

Supplementary data to this article can be found online at https://doi.org/10.1016/j.jenvman.2026.130431.

Data availability

All data used in the article is publicly available.

References

Agarwal, S., Li, B., Qian, W., Ren, Y., Sun, R., 2024. Association between bike-sharing systems and the blood pressure of local citizens: a cross-sectional study in China. BMJ Public Health 2 (2).
Ahn, Y., Okamoto, D., Uejio, C., 2022. Investigating city bike rental usage and wet-bulb globe temperature. Int. J. Biometeorol. 66 (4), 679–690.
An, R., Zahnow, R., Pojani, D., Corcoran, J., 2019. Weather and cycling in New York: the case of Citibike. J. Transport Geogr. 77, 97–112.
Bean, R., Pojani, D., Corcoran, J., 2021. How does weather affect bikeshare use? A comparative analysis of forty cities across climate zones. J. Transport Geogr. 95, 103155.
Bishoi, B., Prakash, A., Jain, V., 2009. A comparative study of air quality index based on factor analysis and US-EPA methods for an urban environment. Aerosol Air Qual. Res. 9 (1), 1–17.
Cao, B., Sun, M., Bardhan, R., 2024. Measuring shaded bike lanes for heat stress mitigation with deep learning: a case study in Amsterdam, Netherlands. Urban Clim. 57, 102126.
Chapman, L., 2007. Transport and climate change: a review. J. Transport Geogr. 15 (5), 354–367.
Chen, Y., Chen, Y., Tu, W., Zeng, X., 2020. Is eye-level greening associated with the use of dockless shared bicycles? Urban For. Urban Green. 51, 126690.
Collins, W.J., Bellouin, N., Doutriaux-Boucher, M., Gedney, N., Halloran, P., Hinton, T., Hughes, J., Jones, C., Joshi, M., Liddicoat, S., 2011. Development and evaluation of an Earth-System model–HadGEM2. Geosci. Model Dev. 4 (4), 1051–1075.
Corcoran, J., Li, T., Rohde, D., Charles-Edwards, E., Mateo-Babiano, D., 2014. Spatio-temporal patterns of a Public Bicycle Sharing Program: the effect of weather and calendar events. J. Transport Geogr. 41, 292–305.
Cortez-Ordonez, A., Vazquez, P.-P., Sanchez-Espigares, J.A., 2024. Features that influence bike sharing demand. Heliyon 10 (18).
Creutzig, F., He, D., 2009. Climate change mitigation and co-benefits of feasible transport demand policies in Beijing. Transport. Res. Transport Environ. 14 (2), 120–131.
Ding, Y., Jian, S., Yu, L., 2025. How to reduce carbon emissions in the urban transportation systems through carbon markets? Balancing the monetary and environmental benefits. Appl. Energy 377, 124454.
Doubleday, A., Choe, Y., Isaksen, T.M.B., Errett, N.A., 2021. Urban bike and pedestrian activity impacts from wildfire smoke events in Seattle, WA. J. Transport Health 21, 101033.
Dunne, J.P., Horowitz, L., Adcroft, A., Ginoux, P., Held, I., John, J., Krasting, J.P., Malyshev, S., Naik, V., Paulot, F., 2020. The GFDL Earth System Model version 4.1 (GFDL-ESM 4.1): overall coupled model description and simulation characteristics. J. Adv. Model. Earth Syst. 12 (11).
El-Assi, W., Salah Mahmoud, M., Nurul Habib, K., 2017. Effects of built environment and weather on bike sharing demand: a station level analysis of commercial bike sharing in Toronto. Transportation 44 (3), 589–613.
Šeparović, L., Alexandru, A., Laprise, R., Martynov, A., Sushama, L., Winger, K., Tete, K., Valin, M., 2013. Present climate and climate change over North America as simulated by the fifth-generation Canadian regional climate model. Clim. Dyn. 41 (11), 3167–3201.
Eren, E., Uz, V.E., 2020. A review on bike-sharing: the factors affecting bike-sharing demand. Sustain. Cities Soc. 54, 101882.
Fishman, E., 2016. Bikeshare: a review of recent literature. Transp. Rev. 36 (1), 92–113.
Gebhart, K., Noland, R.B., 2014. The impact of weather conditions on bikeshare trips in Washington, DC. Transportation 41 (6), 1205–1225.
Gifford, R., Steg, L., 2005. Sustainable transportation and quality of life. J. Transport Geogr. 13 (1), 59–69.
Giorgetta, M.A., Jungclaus, J., Reick, C.H., Legutke, S., Bader, J., Böttinger, M., Brovkin, V., Crueger, T., Esch, M., Fieg, K., 2013. Climate and carbon cycle changes from 1850 to 2100 in MPI-ESM simulations for the Coupled Model Intercomparison Project phase 5. J. Adv. Model. Earth Syst. 5 (3), 572–597.
Giorgi, F., Coppola, E., Solmon, F., Mariotti, L., Sylla, M., Bi, X., Elguindi, N., Diro, G., Nair, V., Giuliani, G., 2012. RegCM4: model description and preliminary tests over multiple CORDEX domains. Clim. Res. 52, 7–29.
Gong, W., Rui, J., Li, T., 2024. Deciphering urban bike-sharing patterns: an in-depth analysis of natural environment and visual quality in New York's Citi bike system. J. Transport Geogr. 115, 103799.
Guo, Y., Yang, L., Chen, Y., 2022. Bike share usage and the built environment: a review. Front. Public Health 10, 848169.
Hastie, T.J., 2017. Generalized additive models. Statistical Models in S, pp. 249–307.
Heaney, A.K., Carrión, D., Burkart, K., Lesk, C., Jack, D., 2019. Climate change and physical activity: estimated impacts of ambient temperatures on bikeshare usage in New York City. Environ. Health Perspect. 127 (3), 037002.
Hesseln, H., Loomis, J.B., González-Cabán, A., Alexander, S., 2003. Wildfire effects on hiking and biking demand in New Mexico: a travel cost study. J. Environ. Manag. 69 (4), 359–368.
Hong, J., McArthur, D.P., Sim, J., Kim, C.H., 2022. Did air pollution continue to affect bike share usage in Seoul during the COVID-19 pandemic? J. Transport Health 24, 101342.
Huang, D., Zhang, Y., Cheng, H., Andrea, C., Shi, J., Chen, C., Teng, Y., Zeng, L., 2024. Evaluating air pollution exposure among cyclists: Real-time levels of PM2. 5 and NO2 and POI impact. Sci. Total Environ. 945, 173559.
Kelly, F.J., Fuller, G.W., Walton, H.A., Fussell, J.C., 2012. Monitoring air pollution: use of early warning systems for public health. Respirology 17 (1), 7–19.
Kharaghani, H., Etemadfard, H., Golmohammadi, M., 2023. Spatio-temporal analysis of precipitation effects on bicycle-sharing systems with tensor approach. J. Geovis Spat. Anal. 7 (2), 30.
Kim, K., 2018. Investigation on the effects of weather and calendar events on bike-sharing according to the trip patterns of bike rentals of stations. J. Transport Geogr. 66, 309–320.
Kou, Z., Cai, H., 2019. Understanding bike sharing travel patterns: an analysis of trip data from eight cities. Phys. Stat. Mech. Appl. 515, 785–797.
Lee, J., Berkelhammer, M., 2025. Evaluating the influence of traffic congestion on surface urban heat island intensity. Geophys. Res. Lett. 52 (16).
Li, Y., Zhu, Z., Kong, D., Xu, M., Zhao, Y., 2019. Learning heterogeneous spatial-temporal representation for bike-sharing demand prediction. Proc. AAAI Conf. Artif. Intell.

Liang, Y., Wang, D., Yang, H., Yuan, Q., Yang, L., 2023. Examining the causal effects of air pollution on dockless bike-sharing usage using instrumental variables. Transport. Res. Transport Environ. 121, 103808.
Mahajan, S., Argota Sánchez-Vaquerizo, J., 2024. Global comparison of urban bike-sharing accessibility across 40 cities. Sci. Rep. 14 (1), 20493.
Mateo-Babiano, I., Bean, R., Corcoran, J., Pojani, D., 2016. How does our natural and built environment affect the use of bicycle sharing? Transport. Res. Pol. Pract. 94, 295–307.
Mo, W., Balen, D., Moura, M., Gardner, K.H., 2018. A regional analysis of the life cycle environmental and economic tradeoffs of different economic growth paths. Sustainability 10 (2), 542.
Noland, R.B., 2021. Scootin'in the rain: does weather affect micromobility? Transport. Res. Pol. Pract. 149, 114–123.
Park, J., Honda, Y., Fujii, S., Kim, S.E., 2022. Air pollution and public bike-sharing system ridership in the context of sustainable development goals. Sustainability 14 (7), 3861.
Pascal, M., Wagner, V., Alari, A., Corso, M., Le Tertre, A., 2021. Extreme heat and acute air pollution episodes: a need for joint public health warnings? Atmos. Environ. 249, 118249.
Perlmutt, L.D., Cromar, K.R., 2019. Comparing associations of respiratory risk for the EPA air quality index and health-based air quality indices. Atmos. Environ. 202, 1–7.
Raza, W., Forsberg, B., Johansson, C., Sommar, J.N., 2018. Air pollution as a risk factor in health impact assessments of a travel mode shift towards cycling. Glob. Health Action 11 (1), 1429081.
Sarkar, A., Lathia, N., Mascolo, C., 2015. Comparing cities' cycling patterns using online shared bicycle maps. Transportation 42 (4), 541–559.
Schepers, P., Fishman, E., Beelen, R., Heinen, E., Wijnen, W., Parkin, J., 2015. The mortality impact of bicycle paths and lanes related to physical activity, air pollution exposure and road safety. J. Transport Health 2 (4), 460–473.
Scinocca, J., Kharin, V., Jiao, Y., Qian, M., Lazare, M., Solheim, L., Flato, G., Biner, S., Desgagne, M., Dugas, B., 2016. Coordinated global and regional climate modeling. J. Clim. 29 (1), 17–35.
Shaheen, S.A., Guzman, S., Zhang, H., 2010. Bikesharing in Europe, the Americas, and Asia: past, present, and future. Transp. Res. Rec. 2143 (1), 159–167.
Skamarock, W.C., Klemp, J.B., Dudhia, J., Gill, D.O., Liu, Z., Berner, J., Wang, W., Powers, J.G., Duda, M.G., Barker, D.M., 2019. A description of the advanced research WRF version 4. NCAR tech. note ncar/tn-556+ str 145 (10.5065).
Swart, N.C., Cole, J.N., Kharin, V.V., Lazare, M., Scinocca, J.F., Gillett, N.P., Anstey, J., Arora, V., Christian, J.R., Hanna, S., 2019. The Canadian Earth system model version 5 (CanESM5. 0.3). Geosci. Model Dev. 12 (11), 4823–4873.
Thornton, M., Shrestha, R., Wei, Y., Thornton, P., Kao, S.-C., 2022. Daymet: Daily Surface Weather Data on a 1-km Grid for North America, Version 4 R1. ORNL DAAC.
Thornton, P.E., Shrestha, R., Thornton, M., Kao, S.-C., Wei, Y., Wilson, B.E., 2021. Gridded daily weather data for North America with comprehensive uncertainty quantification. Sci. Data 8 (1), 190.
Villarrasa-Sapina, I., Toca-Herrera, J.-L., Pellicer-Chenoll, M., Taczanowska, K., Rueda, P., Devís-Devís, J., 2024. Effects of meteorology on bike-sharing: cases of 13 cities using non-linear analyses. Cities 155, 105457.
Wang, M., Zhou, X., 2017. Bike-sharing systems and congestion: evidence from US cities. J. Transport Geogr. 65, 147–154.
Wessel, J., 2020. Using weather forecasts to forecast whether bikes are used. Transport. Res. Pol. Pract. 138, 537–559.
Winkler, L., Pearce, D., Nelson, J., Babacan, O., 2023. The effect of sustainable mobility transition policies on cumulative urban transport emissions and energy demand. Nat. Commun. 14 (1), 2357.
Zheng, R., Liang, Y., Wang, D., Ou, Y., 2025. Shared E-bikes are more resilient than shared bikes to extreme temperatures: evidence from Citi Bike in New York City. J. Transport Geogr. 129, 104412.